Redox Biology 62 (2023) 102706

Contents lists available at ScienceDirect

Redox Biology

journal homepage: www.elsevier.com/locate/redox

MK-886 protects against cardiac ischaemia/reperfusion injury by activating proteasome-Keap1-NRF2 signalling

Kai-Na Shi [1], Pang-Bo Li [1], Hui-Xiang Su, Jing Gao, Hui-Hua Li [*]

Department of Emergency Medicine, Beijing Key Laboratory of Cardiopulmonary Cerebral Resuscitation, Beijing Chao-Yang Hospital, Capital Medical University, Beijing, 100020, China

ARTICLE INFO

Keywords:
MK-886
Myocardial ischaemia/reperfusion injury
Immunoproteasome
Keap1/NRF2
Mitochondrial dynamics
Oxidative stress

ABSTRACT

Oxidative stress is considered a key factor contributing to the initiation and development of cardiac injury following ischaemia–reperfusion (I/R). Arachidonate 5-lipoxygenase (ALOX5) is a rate-limiting enzyme for leukotriene biosynthesis. MK-886 is an inhibitor of ALOX5 that exhibits anti-inflammatory and antioxidant activities. However, the significance of MK-886 in preventing I/R-mediated cardiac injury and the underlying mechanism remain unclear. Cardiac I/R model was produced by ligation/release of the left anterior descending artery. MK-886 (20 mg/kg) was administered intraperitoneally into mice at 1 and 24 h before I/R. Our results indicated that MK-886 treatment significantly attenuated I/R-mediated cardiac contractile dysfunction and decreased the infarct area, myocyte apoptosis, and oxidative stress accompanied with reduction of Kelch-like ECH-associated protein 1 (keap1) and upregulation of nuclear factor erythroid 2-related factor 2 (NRF2). Conversely, administration of the proteasome inhibitor epoxomicin and NRF2 inhibitor ML385 greatly abrogated MK-886-mediated cardioprotection after I/R injury. Mechanistically, MK-886 enhanced the expression of the immunoproteasome subunit β5i, which interacted with keap1 and enhanced its degradation, leading to activation of the NRF2-dependent antioxidant response and improvement of mitochondrial fusion-fission balance in the I/R-treated heart. In summary, our present findings indicated that MK-886 could protect the heart against I/R injury and highlight that MK-886 may represent a promising therapeutic candidate for preventing ischaemic disease.

1. Introduction

Acute myocardial infarction (AMI) is a serious clinical syndrome related to high mortality and morbidity rates. Rapid restoration of blood flow via coronary revascularization is the most effective therapy for AMI, but timely reperfusion may cause cardiac impairment, namely, cardiac ischaemia–reperfusion (I/R) injury. At present, no adequate treatment is available for this disease [1]. Emerging evidence reveals that excessive oxidative stress is closely associated with the pathogenesis of cardiac I/R injury. The Keap1-NRF2-antioxidant response element (ARE) system is a key defence mechanism against oxidative stress and is involved in many diseases, including cancer, neurodegenerative and cardiovascular diseases [2,3]. NRF2 is a master transcription regulator that controls the expression of various endogenous antioxidant enzymes, such as NADPH:quinone oxidoreductase 1 (NQO1), superoxide dismutase (SOD), peroxiredoxin 1 (Prdx1), and glutamate-cysteine ligase (Gclc), by binding to AREs. Accumulating data support that NRF2 plays a critical role in controlling redox homeostasis and protecting against cardiac dysfunction [4,5]. Interestingly, NRF2 activity is modulated by the ubiquitin Cullin3-based E3 ligase Keap1, which increases polyubiquitin chain formation on NRF2 and subsequent degradation of NRF2 by the proteasome [6]. Increasing evidence has suggested that Keap1-NRF2 signalling attenuates oxidative stress and preserves cardiac contractile function following AMI and I/R injury [5,6]. Thus, modulating this pathway is a promising therapeutic chance for the amelioration of I/R-mediated cardiac impairment.

Arachidonate 5-lipoxygenase (ALOX5, also known as 5-LOX or LOG5) is a key enzyme that is necessary for leukotriene biosynthesis from arachidonic acid. ALOX5 critically regulates different types of cell death by increasing inflammation and lipid peroxidation [7]. Moreover, ALOX5 plays fundamental roles in the development of various cardiovascular diseases, including cardiac I/R injury, atherosclerosis, and

* Corresponding author.
E-mail address: hhli1935@aliyun.com (H.-H. Li).
[1] These authors contributed equally to this work.

https://doi.org/10.1016/j.redox.2023.102706
Received 28 February 2023; Received in revised form 9 April 2023; Accepted 18 April 2023
Available online 20 April 2023

abdominal aortic aneurysm, in animal models [8,9]. Therefore, targeting ALOX5 may serve as a promising strategy for treating these diseases. MK-886 has been demonstrated to inhibit ALOX5 activity and exerts anti-inflammatory and antioxidant effects by blocking the infiltration of polymorphonuclear leukocytes into injured tissues [9]. Multiple studies have indicated that MK-886 treatment suppresses inflammation, cancer, renal and hepatic I/R injury, and some CVDs, such as atherosclerosis and hypertension, in various cellular and animal models [9]. However, the functional role of MK-886 in cardiac I/R injury remains to be elucidated. Here, our findings identified MK-886 as a new inducer of cardiac proteasome expression and activity that prevents I/R-mediated cardiac impairment by targeting Keap1-NRF2 signalling and suggest that MK-886 may be useful in protecting against I/R-mediated cardiac dysfunction.

2. Materials and methods

2.1. Mice

Wild-type (WT) mice on the C57BL/6J background were acquired and were kept in the animal center of Beijing Chaoyang Hospital. They were all fed regular mouse food and given unrestricted access to water throughout the study. All procedures were approved by the Committee on the Ethics of Animal Experiments of Beijing Chao-Yang Hospital (2020-Animal-164; approved on March 25, 2020) and conformed to the Guide for the Care and Use of Laboratory Animals published by the U.S. NIH.

2.2. Cardiac I/R model and drug treatment

A mouse cardiac I/R model was established through occlusion and release of the left anterior descending (LAD) coronary artery based on previous protocols [10,11]. In brief, male mice aged 10 weeks (22 ± 2 g) were anaesthetized by inhalation of isoflurane (1.5–2.0%). The LAD artery was reversibly ligated for 30 min (ischaemia) followed by 24 h of reperfusion. The controls underwent the same procedure without artery occlusion (sham group). MK-886 (HY-14116, MCE), epoxomicin (a proteasome inhibitor, HY-13821, MEC) and ML385 (an NRF2 inhibitor, HY-100523, MEC) were dissolved in DMSO and further diluted in corn oil. To test the impact of MK-886 on cardiac impairment following I/R, 24 animals were grouped randomly into four groups (n = 6 per group): the sham + vehicle, sham + MK-886, I/R + vehicle, and I/R + MK-886. The mice were intraperitoneally administered MK-886 (20 mg/kg) 2 and 24 h before I/R surgery. To evaluate the effect of epoxomicin (Epox) and ML-385 on I/R-mediated cardiac injury, 42 mice were grouped randomly into the following groups (n = 6 each group): the I/R + vehicle, I/R + MK-886, I/R + vehicle + Epox, I/R + MK-886+Epox, I/R + vehicle + ML385, and I/R + MK-886 + ML385. The mice were intraperitoneally administered MK-886 (20 mg/kg) and epoxomicin (1 mg/kg) or ML385 (30 mg/kg) at 2 and 24 h before surgery [12,13]. All animals were sacrificed with an injection of tribromoethanol at (500 mg/kg) 24 h following surgery. Heart tissues and blood samples were collected for further experiments.

2.3. Echocardiographic assessment

All animals (n = 6) were anaesthetized with isoflurane at dosage of 1.5% to determine the effect of MK-886 on heart function following sham surgery or I/R. Mouse heart rate was not greatly impacted by anaesthesia. A Vevo 2100 high-resolution imaging machine was used for echocardiography to evaluate heart structure and left ventricular (LV) contractile function (Visual Sonics Inc.). As described in previous protocols, echocardiographic parameters, i.e., ejection fraction (EF%), fractional shortening (FS%), LV internal diameter at end-diastole (LVIDd) and end-systole (LVIDs), LV anterior wall thickness at end-diastole (LVAWd) and end-systole (LVAWs), were analysed [10,11].

2.4. Infarct area analysis

All mice (n = 6) were overdosed with 100 mg/kg tribromoethanol by intraperitoneal injection, followed by transcardial perfusion with saline solution. After religation of LAD artery, approximately 900 μl of Evans blue dye (1%) was injected into the LV. Then, all hearts were frozen at −20 °C for 15–20 min. They were cut into 4 at a thickness of approximately 2 mm. The heart slices were stained with 1% 2,3,5-triphenyltetrazolium chloride solution (TTC) for 30 min (37 °C) to assess the infarct area and were then incubated in 4% paraformaldehyde for 24 h. Three main zones in the stained heart slices were observed, i.e., a non-ischaemic area (blue), an infarcted area (white), and an ischaemic area (red), as previously described [10,11]. All slices were evaluated with ImageJ software. ImageJ software was used to examine each section. The formula for calculating the area at risk (AAR) was (infarct area + ischaemic area)/total LV area, and cardiac infarct area was expressed as the percentage of infarct area/total LV area.

2.5. TUNEL assay and measurement of reactive oxygen species levels

Heart tissues were incubated in 20% sucrose solution and routinely embedded in OCT compound (#4583, SAKURA). Cryosections (4 μm) were pretreated using 0.2% Triton X-100. Apoptotic cardiomyocytes were visualized using a commercial reagent kit (red, #12156792910, Roche) following the protocols of manufacturer. Cardiomyocytes were identified with an α-actinin antibody (green, #11313-2-AP, Proteintech). Nuclei were stained with DAPI (blue, #C1006, Beyotime) as previously described [10,11]. The images of $TUNEL^+$ myocytes were photographed by a fluorescence microscope (DM2500, Leica, Germany) at wavelengths of excitation/emission (450/515 nm), respectively. For detection of reactive oxygen species (ROS) levels, 4 μm thick cryosections were pretreated with 0.5% Triton and were then incubated with 1 μM dihydroethidium (DHE) in PBS at 37 °C for 30 min. The images of 5 random fields were obtained for each heart by a fluorescence microscope at wavelengths of excitation/emission (560/620 nm), respectively. The percentage of $TUNEL^+$ apoptotic myocytes and DHE intensity were evaluated by ImageJ software (NIH).

2.6. Measurement of LDH activity

Serum samples were diluted 80 times with distilled water, and the level of lactate dehydrogenase (LDH) was determined with a commercial kit at a wavelength of 450 nm following manufacturer's protocol (#A020-2-2, Jiancheng Bioengineering Institute, Nanjing).

2.7. Detection of MDA and SOD activities

Malondialdehyde (MDA) and SOD activity in serum was measured with commercial kits (#S0131, #S0101 M, Beyotime) at a wavelength of 532 nm or 450 nm, respectively, following the manufacturer's protocols.

2.8. Analysis of cardiac ATP content

Ten milligrams of heart tissue (n = 6) was ground in 100 μl ATP reaction solution and then centrifuged at 12,000×*g* for 5 min. The isolated supernatants were mixed with ATP working solution at RT for 3–5 min. Cardiac ATP levels were measured with an automatic microplate reader (#30086376, model: Spark) using an ATP Assay Kit (#S0027, Beyotime).

2.9. Immunoblotting

Total protein was purified from the heart border zone of mice following sham surgery or I/R (n = 4) using RIPA buffer (#P0013C, Beyotime). The levels of proteins were determined with a commercial kit following the manufacturer's protocol (#23225, Thermo). Equal

proteins (40–50 μg) were separated by 10% sodium dodecylsulfate-polyacrylamide (SDS)-polyacrylamide gel electrophoresis (PAGE), transferred to PVDF membranes, and then mixed with primary antibodies (Table S1) overnight. Densitometric analysis of all protein bands was analysed with ImageJ software, and each protein band density was normalized to the level of GAPDH as reported previously [10].

2.10. Quantitative real-time PCR

Total RNA was purified from heart border zone tissues obtained from sham and I/R mice (n = 6) with TRIzol (#9109, TaKara). The cDNA was synthesized with total RNA (1 μg) using reverse transcription (RT) enzyme mix (#RR047A, TAKARA). The mRNA levels of Bax, Bcl-2, interleukin (IL)-1β, IL-6, NOX2, NOX4, TNF-α, NQO1, Gclc, SOD1, and Prdx1 were measured by PCR, which was performed with a thermocycler (Bio-Rad), and were normalized to the level of GAPDH. The primers are provided in Table S2.

2.11. Measurement of three proteasome activities

Total protein was isolated from the heart tissues of sham and I/R mice. A total of 20 μg lysate proteins were added to 50 μl of reaction buffer that contains three fluorogenic peptides, including *Z*-nLPnLD-Glo™ (40 μM), *Z*-LRR-Glo™ (30 μM), or Suc-LLVY-Glo™ (40 μM), and reacted at RT for 10 min. Proteasomal activities (caspase-like, trypsin-like, and chymotrypsin-like) in the tissues were evaluated using Proteasome-Glo assay kit following the manufacturer's instructions (Promega) as previously reported [14]. The fluorescence intensities

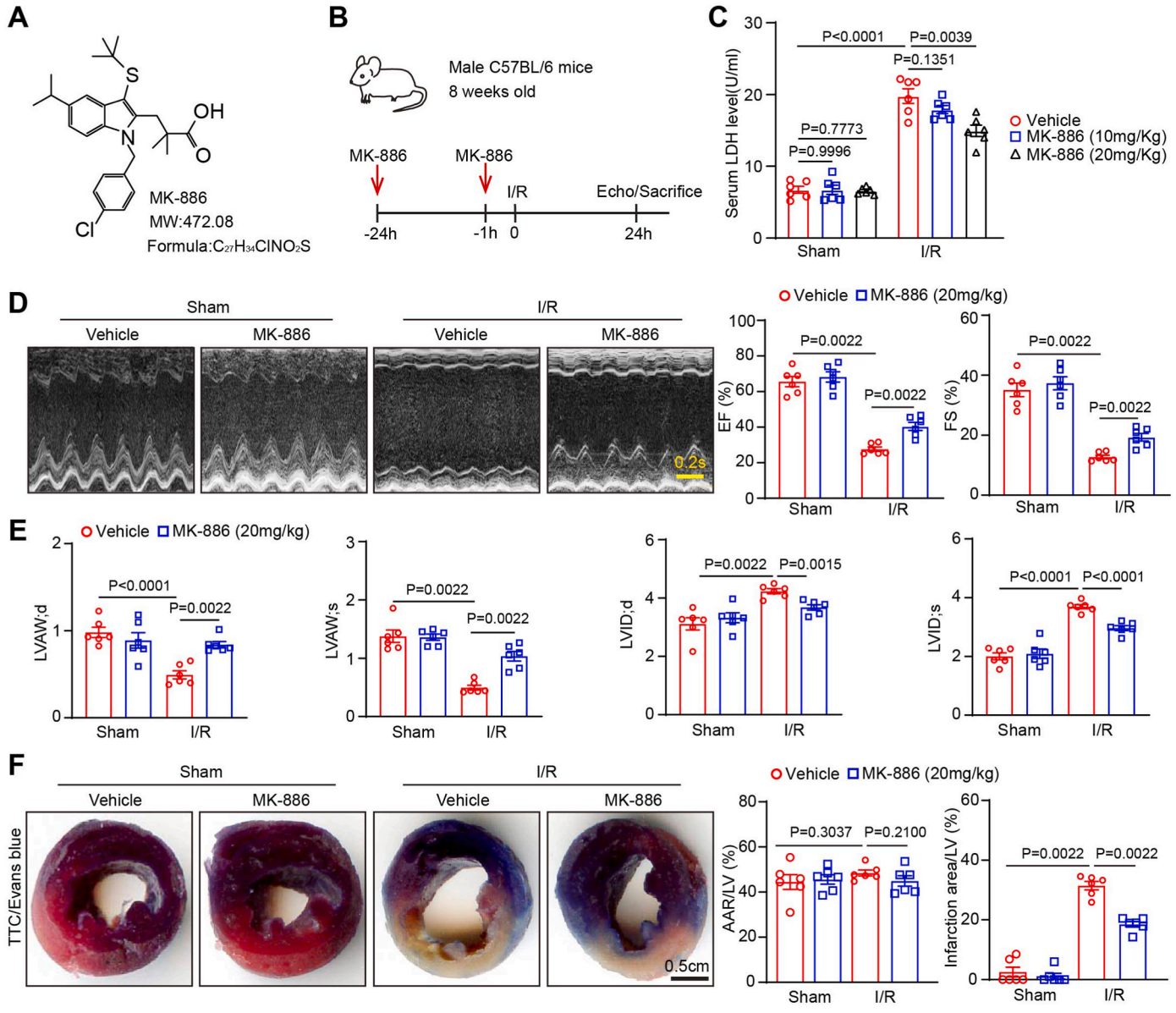

Fig. 1. MK-886 alleviates I/R-induced reduction of cardiac function.
(A) Chemical structure and molecular weight of MK-886. **(B)** Schematic design of the experiments. Male mice were pretreated with MK-886 (10 or 20 mg/kg) and then subjected to ischaemia/reperfusion (I/R) for 24 h. **(C)** Measurement of serum LDH activity in the border zone of ischaemic heart tissues by assay kits (n = 6). **(D)** Echocardiographic images of the left ventricle (LV, left). Scale bar: 0.2 s. Quantification of ejection fraction (EF%) and fractional shortening (FS%) (right, n = 6). **(E)** Quantification of echocardiographic parameters of LV structure, including LV anterior wall thickness at end-diastole (LVAWd) and end-systole (LVAWs), LV internal diameter at end-diastole (LVIDd) and end-systole (LVIDs) (n = 6). **(F)** Images of Evans blue and TTC double staining of the cardiac infarct area (left). Quantitative analysis of the infarction area/LV area and AAR/LV area ratios (n = 6, right). The data are expressed as the mean ± SEM, and n represents the number of mice in each group. (For interpretation of the references to colour in this figure legend, the reader is referred to the Web version of this article.)

were measured with an automatic microplate reader (Spark).

2.12. Statistics

The data are reported as the mean ± SEM. All results were analysed with SPSS (21.0, IBM Corp) or Prism (version 9.0, La Jolla) software. Normality plots and Levene variance homogeneity tests were used to assess data normality, and bifurcation homogeneity analysis of the data was performed. For comparisons of multiple groups, one-way analysis of variance was used, with Bonferroni's or Dunnett's multiple-comparisons test for normally distributed results or the Mann-Whitney test for non-normally distributed results. A P value < 0.05 was considered to indicate statistical significance.

3. Results

3.1. MK-886 alleviates I/R-mediated cardiac infarction and functional decline

To investigate the impact of MK-886 on I/R-triggered cardiac injury, we first pretreated WT mice with MK-886 at a dosage of 10 or 20 mg/kg and subjected them to I/R as described in previous studies (Fig. 1A–B) [15,16]. At 24 h after treatment, measurement of LDH activity (a marker of cardiac injury) indicated that neither dose had a significant cardiotoxic effect in sham mice, whereas 20 mg/kg MK-886 significantly reduced LDH activity in the hearts of I/R mice (Fig. 1C). Thus, we selected 20 mg/kg as the MK-886 dose for the following experiments. At 24 h after I/R, echocardiographic measurements indicated that the I/R-mediated reduction in cardiac contractility, as evidenced by a reduced EF% and FS%, was reversed in MK-886-administered mice compared with vehicle-administered mice (Fig. 1D, Table S3). Consistently, compared with vehicle treatment, MK-886 administration dramatically ameliorated I/R-triggered cardiac structural changes, as indicated by an increases in LVAWd, LVAWs, LVIDd, and LVIDs (Fig. 1E). Moreover, I/R injury significantly increased the cardiac infarct area (assessed by TTC/Evans blue staining), as reflected by an increased infarct area/LV area ratio, in vehicle-administered mice. Conversely, this increase was markedly suppressed in MK-886-treated mice (Fig. 1F).

3.2. MK-886 suppresses I/R-mediated myocyte apoptosis, inflammation, and oxidative stress

Since MK-886 exerts antioxidant and anti-inflammatory effects, we then examined whether MK-886 affects cardiomyocyte apoptosis, oxidative stress and inflammatory cytokines, which are the main contributors to cardiac dysfunction, in the hearts of I/R mice. Cardiomyocyte apoptosis (TUNEL staining), the percentage of Mac-2^{+} macrophages, and ROS generation (DHE staining) were markedly increased in I/R mice compared with sham mice following vehicle administration, but the I/R-induces increases in these measures were dramatically blocked in MK-886-treated mice (Fig. 2A–C). Accordingly, the Bax/Bcl-2 protein and mRNA ratios, markers of apoptosis, the mRNA expression levels of proinflammatory markers (IL-1β, IL-6 and TNF-α) and NADPH oxidases (NOX2 and NOX4) and the serum level of MDA (an oxidative stress marker) were all lower in MK-886-pretreated mice than in vehicle-pretreated mice after I/R (Fig. 2D–H). In contrast, cardiac ATP levels and serum levels of SOD (an antioxidative enzyme) were higher in MK-886-pretreated mice than in vehicle-pretreated controls following I/R (Fig. 2H–I). Collectively, these results reveal that MK-886 exerts a cardioprotective effect during I/R injury.

3.3. MK-886 targets Keap1 degradation, leading to activation of NRF2 signalling and improvement of mitochondrial dynamics

Excessive oxidative stress is a critical factor contributing to cardiac I/R impairment. The Keap1-NRF2-ARE axis is considered a key signalling pathway in abating the detrimental effects of I/R-induced oxidative stress on cardiac function [2]. Then, we determined whether MK-886 influences this pathway in the hearts of I/R mice. Interestingly, immunoblotting that Keap1 protein expression was significantly increased while NRF2 protein expression was downregulated in the I/R mice compared with the sham mice at 24 h after surgery, but this change was markedly reversed in MK-886-pretreated mice (Fig. 3A). Notably, neither I/R nor MK-886 altered keap1 mRNA levels (Fig. 3B), suggesting that MK-886 regulates Keap1 at the protein level. Next, we examined the mRNA expression of several genes downstream of the Keap1-NRF2-ARE axis (NQO1, Gclc, SOD1, and Prdx1), which exert antioxidant effects in cardiac I/R injury. As expected, qPCR analysis showed that the I/R-mediated downregulation of NQO1, Gclc, SOD1, and Prdx1 mRNA expression in heart tissues was dramatically restored in MK-886-pretreated mice compared with vehicle-pretreated controls (Fig. 3C), suggesting that MK-886 can increase NRF2 transcription by reducing keap1 stability.

Moreover, several studies suggest that Keap1-NRF2-ARE signalling is involved in modulating mitochondrial dynamics and function [17–19]; therefore, we tested the impact of MK-866 on mitochondrial dynamics-related protein expression in the heart. Immunoblotting showed that the I/R-mediated enhancement of Drp1 protein and reduction of Mfn1/2 protein were also significantly attenuated in the hearts of MK-886-pretreated I/R model mice (Fig. 3D). Therefore, these data demonstrate that MK-886 has the ability to improve the mitochondrial fission/fusion balance via Keap1-NRF2 signalling.

3.4. MK-886 increases cardiac immunoproteasome subunit expression and activity

In addition to the degradation of NRF2 being mediated by the Keap1-Cul3-Rbx1 complex, Keap1 itself is negatively regulated via ubiquitination and degradation by the proteasome [20–22]. Given that MK-886 reduced Keap1 protein levels but not mRNA levels in the hearts of I/R mice (Fig. 3A–B), we presumed that MK-886-mediated stabilization of the Keap1 protein was regulated by the proteasome in the heart. Therefore, we first evaluated the impact of MK-886 on proteasome activity and discovered that proteasome trypsin-like and chymotrypsin-like activities but not caspase-like activity was significantly increased in heart tissues in the MK-886-administered mice compared with the vehicle-administered mice following sham surgery and I/R (Fig. 4A). Interestingly, the mRNA levels of three constitutive subunits (β1, β2, and β5) and an immunosubunit (β1i) were similar between vehicle- and MK-866-administered mice following sham surgery and I/R (Fig. 4B). However, the I/R-mediated decrease in β2i and β5i mRNA expression levels was markedly inhibited in the heart tissues of MK-886-administered mice compared to those of vehicle-pretreated mice following I/R (Fig. 4B). Furthermore, immunoblotting validated the effect of MK-886 in altering β2i and β5i protein levels in the I/R heart tissues of mice (Fig. 4C). Thus, these results indicate that MK-886 is an inducer of cardiac β2i and β5i expression.

3.5. β5i interacts with Keap1 and promotes its degradation in the heart

To test whether MK-886 regulates the degradation of Keap1 by enhancing immunoproteasome activity, we performed coimmunoprecipitation (Co-IP) with an *anti*-keap1 antibody using the heart tissues of vehicle- and MK-886-treated mice. As expected, the I/R group showed considerably higher ubiquitinated Keap1 protein levels than the sham control group. Conversely, ubiquitinated Keap1 protein levels were markedly decreased in the hearts of MK-886-pretreated mice (Fig. 4D), indicating that MK-886 increased proteasome activity to promote the degradation of ubiquitinated Keap1 in the I/R hearts.

To explore how β2i and β5i regulate Keap1 degradation in the I/R hearts, we performed coimmunoprecipitation (IP) with IgG control, *anti*-β5i, *anti*-β2i or *anti*-keap1 antibody and examined whether there was an

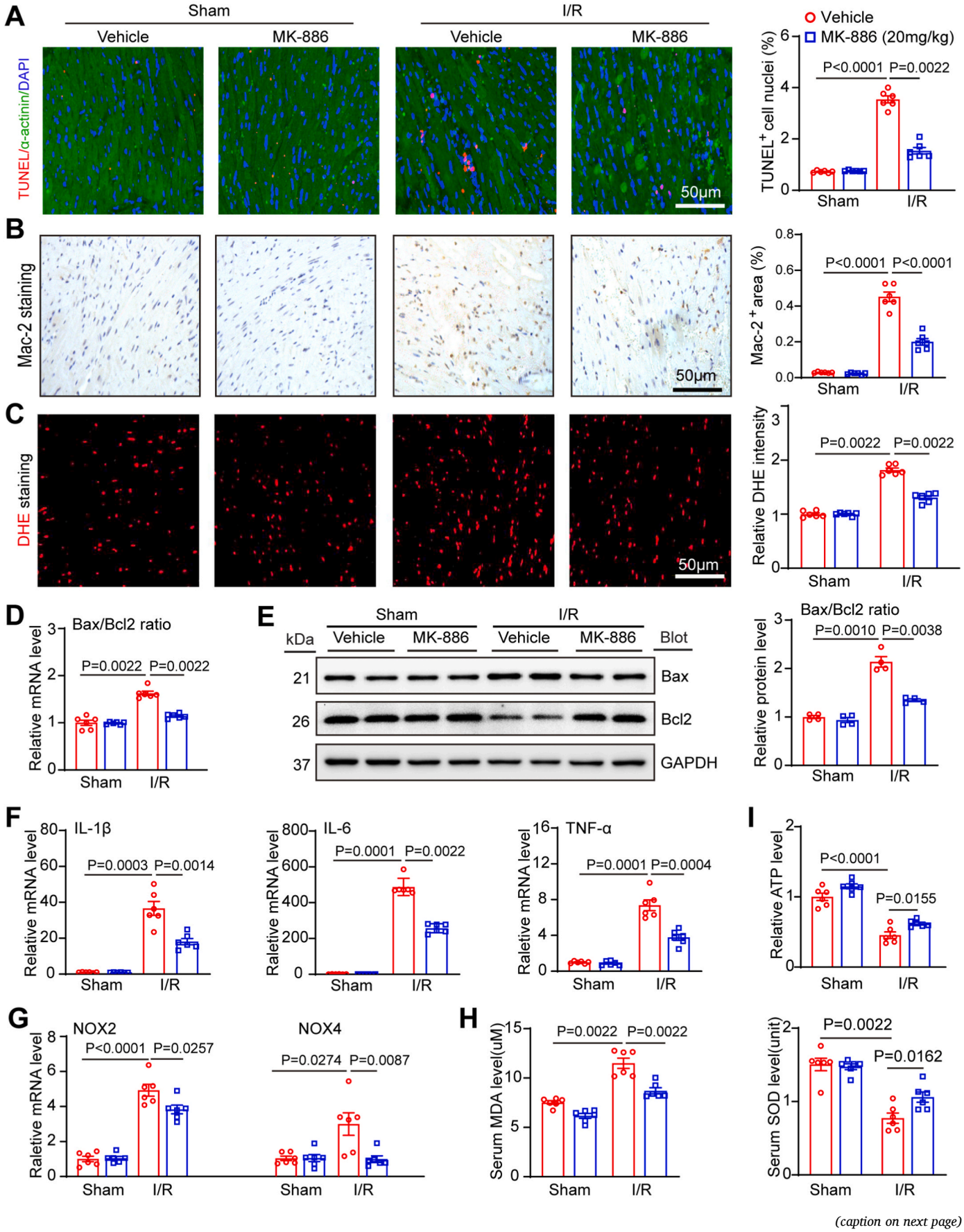

(caption on next page)

Fig. 2. MK-886 inhibits I/R-induced cardiomyocyte apoptosis, inflammation and oxidative stress.
(A) Male mice were pretreated with MK-886 (20 mg/kg) and then subjected to I/R for 24 h. TUNEL (red), α-actinin (green), and DAPI (blue) staining of heart slices (left). The percentage of TUNEL$^+$ myocyte nuclei (right, n = 6). **(B)** Immunohistochemical staining of heart slices with an anti-Mac-2 antibody (left) and quantification of the Mac-2$^+$ area (right, n = 6). **(C)** Dihydroethidium (DHE) staining of heart slices (left) and quantification of the fluorescence intensity (right, n = 6). Scale bar: 50 μm. **(D)** qPCR analysis of Bax and Bcl-2 mRNA levels in the border zone of the ischaemic heart. The data are presented as the Bax/Bcl-2 ratio (n = 6). **(E)** Immunoblot analysis of Bax and Bcl2 protein levels in ischaemic heart tissues (left) and quantification of relative protein levels (right, n = 4). The results are expressed as the Bax/Bcl-2 ratio. **(F–G)** qPCR analysis of IL-1β, IL-6, TNF-α, NOX2, and NOX4 mRNA levels in the ischaemic heart (n = 6). **(H)** Detection of serum malondialdehyde (MDA) and superoxide dismutase (SOD) levels (n = 6). **(I)** Relative ATP content in the ischaemic heart. The data are expressed as the mean ± SEM, and n represents the number of mice in each group. (For interpretation of the references to colour in this figure legend, the reader is referred to the Web version of this article.)

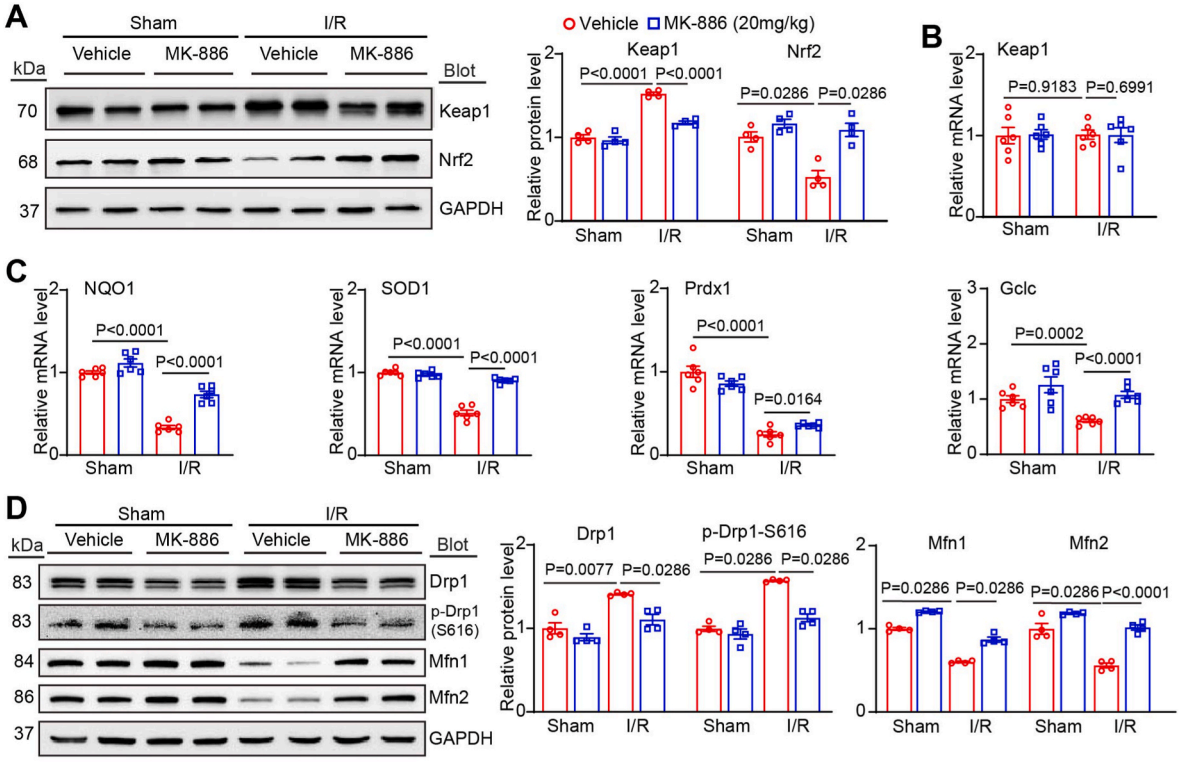

Fig. 3. Effect of MK-886 on the cardiac levels of Keap1, NRF2 and mitochondrial dynamics-related proteins.
(A) Male mice were pretreated with MK-886 (20 mg/kg) and then subjected to I/R for 24 h. Immunoblot analysis of Keap1 and NRF2 protein levels in the border zone of ischaemic heart tissues (left) and quantification of relative protein levels (right, n = 4). **(B)** qPCR analysis of Keap1 mRNA levels in heart tissues (n = 6). **(C)** qPCR analysis of NADPH:quinone oxidoreductase 1 (NQO1), superoxide dismutase 1 (SOD1), peroxiredoxin 1 (Prdx1) and glutamate cysteine ligase (Gclc) mRNA levels in ischaemic heart tissues (n = 6). **(D)** Immunoblot analysis of phosphorylated (p)-Drp1 (S616), Drp1, Mfn1 and Mfn2 protein levels in ischaemic heart tissues (left) and quantification of relative protein band densities (right, n = 4). GAPDH was used as an internal control. The data are expressed as the mean ± SEM, and n represents the number of mice in each group.

interaction between the endogenous immunoproteasome subunit β5i or β2i and Keap1. Immunoblotting indicated that β5i but not β2i interacted with Keap1 (Fig. E–F). Together, these data indicate that MK-886 mediates the degradation of ubiquitinated Keap1 by increasing the interaction of β5i and Keap1 in the heart following I/R.

3.6. Blockage of proteasome activity abolishes MK-886-mediated degradation of Keap1 and prevents cardiac I/R injury

To evaluate whether proteasome activity is involved in the impact of MK-886 on keap1 degradation and cardioprotection against I/R damage, we first analysed the effect of different doses of the proteasome inhibitor Epox, which mainly covalently binds to and targets the β5 subunit, on cardiac injury in mice as previously described [23,24]. Neither dose (0.5 nor 1.0 mg/kg) had significant cardiotoxic effects, as measured by LDH activity (Fig. S1A), and Epox dose-dependently decreased chymotrypsin-like activity but did not significantly change caspase-like or trypsin-like activity in the heart (Fig. S1B). Then, we pretreated mice with Epox (1 mg/kg) and MK-886 (20 mg/kg) prior to I/R. At 24 h after treatment, Epox dramatically decreased chymotrypsin-like activity, but caspase-like and trypsin-like activity was not different among the groups (Fig. S1C). Consistent with the data shown in Fig. 1D–F and Fig. 2, compared with vehicle administration, MK-886 administration greatly suppressed the I/R-induced reduction in the EF% and FS% and increases in the infarct area/LV area ratio, LV chamber dilation (decreased LVIDd and LVIDs), percentage of TUNEL$^+$ apoptotic myocytes, and ROS production as well as the Bax/BCl2 ratio and NOX4 mRNA expression in the heart (Fig. 5A–F). Conversely, these protective actions were substantially abrogated in Epox- and MK-886-cotreated mice (Fig. 5A–F). Moreover, MK-886 significantly reversed the I/R-induced enhancement of Keap1 protein expression and decrease of NRF2 protein leve, which led to upregulation in the mRNA expression of NQO1, Gclc, SOD1, and Prdx1, an increase in serum SOD levels and a reduction in serum MDA levels in the heart (Fig. 5G–I). However, these changes were fully abolished in Epox- and MK-886-cotreated mice (Fig. 5G–I). Consistently, MK-886 treatment

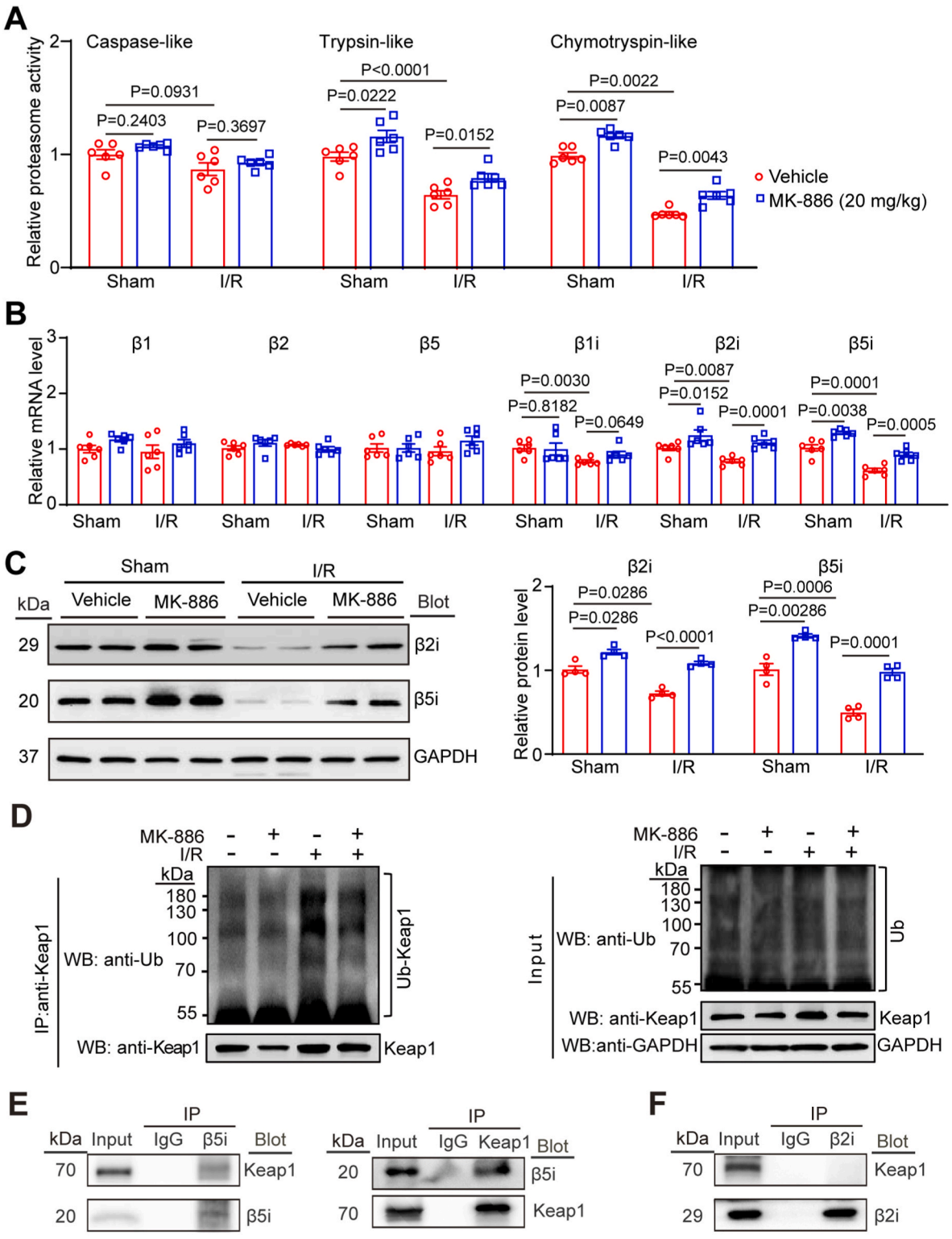

Fig. 4. MK-8886 enhances immunoproteasome subunit expression and activity in the heart after I/R.
(A) Male mice were pretreated with MK-866 (20 mg/kg) and then subjected to I/R for 24 h. Measurement of proteasome caspase-like, trypsin-like and chymotrypsin-like activities in the border zone of ischaemic heart tissue (n = 6). **(B)** qPCR analyses of the mRNA expression of three constitutive proteasome subunits (β1, β2, and β5) and three immunoproteasome subunits (β1i, β2i, and β5i) in ischaemic heart tissues (n = 6). **(C)** Immunoblot analysis of the protein levels of the immunoproteasome subunits (β2i and β5i) in ischaemic heart tissue (left). Quantification of relative protein band densities (right, n = 4). GAPDH was used as an internal control. **(D)** At 24 h after sham surgery or I/R, lysates isolated from the heart tissues of vehicle- and MK-886-treated mice were immunoprecipitated with an *anti*-Keap1 or *anti*-ubiquitin (Ub) antibody. Immunoblot analysis of ubiquitin-conjugated Keap1 (left) and the input for each protein (right). **(E-F)** Interactions between endogenous β5i and Keap1 proteins were examined. Lysates isolated from WT heart tissues were immunoprecipitated with IgG control, *anti*-β5i, *anti*-β2i, or *anti*-Keap1 antibody, and immunoblot analysis of Keap1, β5i, and β2i proteins was performed with an *anti*-Keap1, *anti*-β5i, or *anti*-β2i antibody. The data are expressed as the mean ± SEM, and n represents the number of mice in each group.

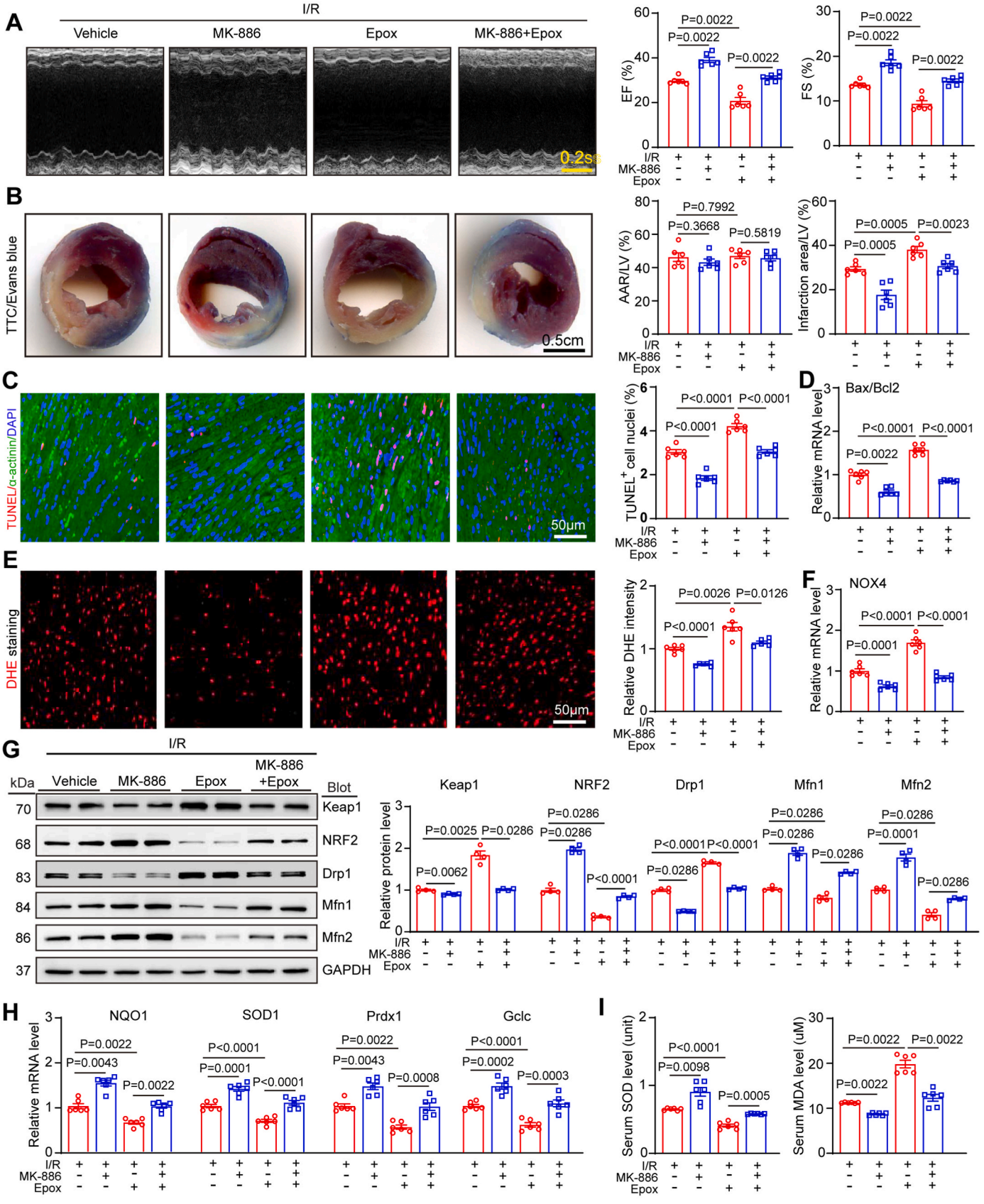

(caption on next page)

Fig. 5. Inhibition of proteasome activity abrogates MK-886-mediated cardioprotection and activation of Keap1-NRF2 signalling following I/R injury.
(A) Male mice were pretreated with MK-886 (20 mg/kg) and epoxomicin (Epox, 1 mg/kg) and then subjected to I/R for 24 h. Echocardiographic images of the left ventricle (left). Scale bar: 0.2 s. Quantification of EF% and FS% (right, n = 6). **(B)** Images of Evans blue and TTC staining (left) for analysis of the infarct size and quantitative analysis of the infarction area/left ventricular (LV) area and area at risk (AAR)/LV area ratios (right, n = 6). **(C)** Images of TUNEL (red), α-actinin (green), and DAPI (blue) staining of cardiac slices (left) and the percentage of TUNEL$^+$ nuclei (right, n = 6). **(D)** qPCR analyses of Bax and Bcl-2 mRNA levels in the border zone of the ischaemic heart (n = 6) and quantification of the relative Bax/Bcl-2 ratio. **(E)** DHE staining of cardiac slices (left) and quantification of the fluorescence intensity indicating the ROS level (right, n = 6). Scale bar: 50 μm. **(F)** qPCR analyses of NOX4 mRNA levels (n = 6). **(G)** Immunoblot analysis of Keap1, NRF2, Drp1 and Mfn1/2 protein levels and quantification of relative protein band densities (right, n = 4). GAPDH was used as an internal control. **(H)** qPCR analyses of NQO1, SOD1, Prdx1 and Gclc mRNA levels (n = 6). **(I)** Measurement of serum SOD and MDA levels by assay kits (n = 6). The data are expressed as the mean ± SEM, and n represents the number of mice in each group. (For interpretation of the references to colour in this figure legend, the reader is referred to the Web version of this article.)

resulted in a decrease in Drp1 protein level and an increased in Mfn1/2 protein levels in the heart, and these effects were markedly attenuated in Epox- and MK-886-cotreated mice (Fig. 5G). In addition, Epox had a similar preventive effect on MK-886-mediated cardioprotection in mice (Fig. 5A–I). Collectively, our findings indicate that MK-886 protects against I/R-induced cardiac injury by enhancing immunoproteasome activity *in vivo*.

3.7. Pharmacological inhibition of NRF2 abrogates MK-886-mediated protection against cardiac I/R imparment

To further confirm whether NRF2 mediates the preventive effect of MK-886 against I/R-mediated decrease in cardiac function *in vivo*, we pretreated WT mice with ML385 (a specific NRF2 inhibitor, 30 mg/kg) [25] and MK-886 (20 mg/kg), and subsequently subjected them to I/R for 24 h. Immunoblotting indicated that NRF2 protein expression was upregulated in the MK-886-administered mice compared with the vehicle-administered controls, but the increase was markedly inhibited in ML385-pretreated mice (Fig. 6G). Moreover, consistent with the findings shown in Fig. 5, the MK-886-mediated enhancement of cardiac contractile function (FS% and FS%) and decreases in the infarct size, LV chamber dilation, the percentage of TUNEL$^+$ apoptotic myocytes, and ROS generation as well as the Bax to Bcl-2 ratio and NOX4 mRNA level in heart tissue were significantly ameliorated in ML385-and MK-886-cotreated mice following I/R (Fig. 6A–F). Furthermore, compared with vehicle-treated controls, MK-886-treated mice had a lower Drp1 protein level and higher Mfn1/2 protein levels, and these changes were reversed in the hearts of ML385-and MK-886-cotreated mice (Fig. 6G). Accordingly, the MK-886-induced increases in the mRNA levels of NQO1, Gclc, SOD1, and Prdx1 and serum SOD concentration and reduction in serum MDA level in heart tissue was markedly attenuated in ML385-and MK-886-cotreated mice (Fig. 6H–I). Thus, these findings indicate that MK-886 ameliorates cardiac I/R injury by enhancing NRF2 activation.

4. Discussion

Here, we identified a novel role for MK-886 in preventing I/R-mediated cardiac damage and dysfunction. MK-886 acts as a proteasome enhancer to upregulate the expression of the immunosubunit β5i, which interacts with keap1 and promotes its degradation, leading to NRF2-dependent activation of antioxidant enzymes, thereby reducing oxidative stress, mitochondrial dynamic imbalance and subsequent cardiac damage (Fig. 7). Therefore, MK-886 may represent a promising therapeutic agent for the amelioration of I/R-triggered cardiac dysfunction in patients.

The molecular mechanisms of cardiac I/R injury are complex. Excessive ROS production and inflammation are the major causes of cardiomyocyte death and dysfunction after reperfusion. 5-LOX catalyses arachidonic acid (AA) to form leukotrienes, which are crucial for the generation of ROS and MDA in various immune and inflammatory diseases [7,8]. The functional role of 5-LOX in the pathogenesis of I/R-induced cardiac injury has been explored in various experimental models, but the conclusions are inconsistent due to cell type and organ specificity [9,26–28]. Interestingly, several 5-LOX inhibitors, such as zileuton, A-64077, and ardisiaquinone A, have been found to protect against ischaemic injury in various organs and tissues in animals [27,29]. Notably, MK-886 is another inhibitor of 5-LOX that has anti-inflammatory and antioxidant effects [30], and can effectively suppress artery injury, pulmonary hypertension, cardiac injury following transplantation, and renal, hepatic and intestine I/R injury by interfering with inflammation, oxidative stress and apoptosis related signalling pathways [31–35]. For example, MK-886 treatment significantly improves angioplasty-induced arterial injury by reducing deposition of platelets and neutrophils, vasoconstrictive response, and synthesis of leukotriene B4 [31]. Administration of MK-886 can limit global cardiac I/R damage following heart transplantation through inhibiting upregulation of cardiac IL-1β, TNF-α, and ICAM-1 levels [32]. Furthermore, MK-886 treatment greatly ameliorates pulmonary hypertension triggered by angiotensin II or hypoxia in vitro and *in vivo* [33]. MK-886 administration dramatically improves I/R-mediated impairment of kidney, liver and intestine associated with lower levels of apoptosis, MDA, TNF-α, IL-6, and creatinine in serum or tissues [34,35]. However, whether MK-886 is able to prevent I/R-triggered cardiac dysfunction and the potential mechanism are largely unclear. Here, we identified for the first time that MK-886 can ameliorate I/R-triggered cardiac impairment by increasing antioxidant activity and mitochondrial dynamic balance via the immunoproteasome-Keap1-NRF2 pathway.

The standard 20S proteasome contains three constitutive β1, β2 and β5 subunits, which exhibit three types of caspase-like, trypsin-like and chymotrypsin-like activities. The immunoproteasome is inducible under inflammatory conditions and comprises three inducible β-subunits (also known as immunoproteasome subunits; β1i, β2i and β5i, which are involved in the inflammatory reaction and various immune diseases [36]. In particular, our recent studies identified that the expression levels of immunosubunits such as β2i and β5i are markedly increased in cardiovascular tissues and cells as well as in human patients and that these subunits are able to target different substrates, including ATG5, PTEN, ATRAP, IKBα, and SOCS3, thereby regulating apoptosis, autophagy, oxidative stress, and inflammation in animal models of cardiac hypertrophic remodelling, myocardial dysfunction, atrial fibrillation and abdominal aortic aneurysm [37–41]. Although numerous proteasome inhibitors, such as bortezomib (velcade), have been developed and can be safely administered to treat blood tumours with few side effects, very few molecules have been identified as potentially effective proteasome enhancers to date. Recently, we identified that ursolic acid (UA) is a new enhancer of immunoproteasome subunit expression that can prevent cardiac I/R injury [14]. Furthermore, several signalling mediators, such as STAT and cAMP-response element-binding protein (CREB), can increase immunoproteasome subunit transcription [42]. To elucidate how MK-886 upregulates β5i expression, we used the bioinformatic program TargetScan to predict the STAT3 binding site in the β5i promoter (Fig. S2A). Immunoblot analysis indicated that I/R markedly upregulated the p-STAT3 level, but MK-886 greatly reversed this effect (Fig. S2B), suggesting that STAT3 may be involved in regulating β5i expression in the I/R hearts. Thus, our data show for the first time that MK-886 may act as a new inducer of β5i expression, likely by

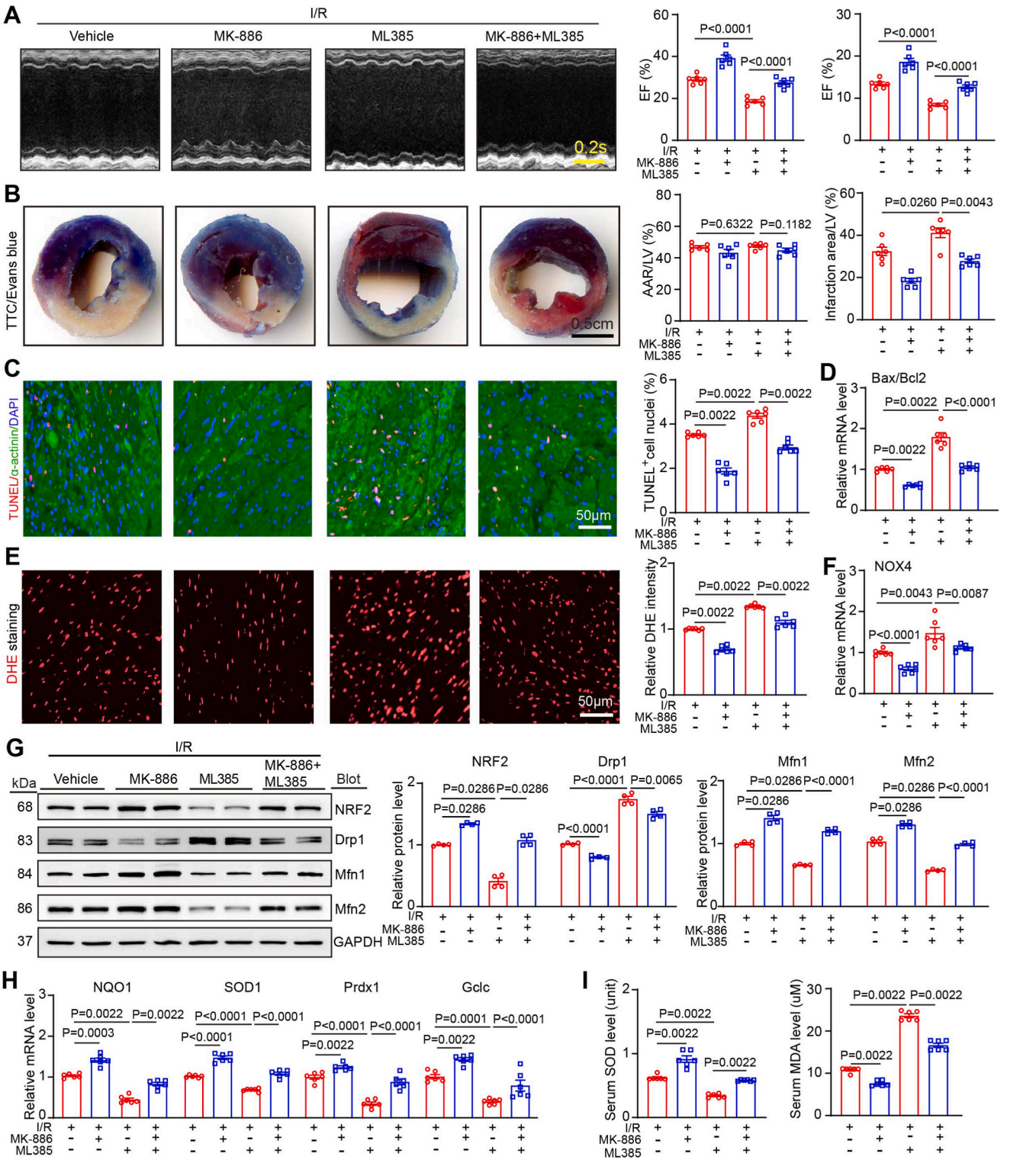

Fig. 6. Blockage of NRF2 transcription factor activity abolishes MK-886-mediated cardioprotection against I/R injury.
(A) Male mice were pretreated with MK-886 (20 mg/kg) and ML385 (30 mg/kg) and then subjected to I/R for 24 h. Echocardiographic images of the left ventricle (left). Scale bar: 0.2 s. Quantification of EF% and FS% (right, n = 6). **(B)** Images of Evans blue and TTC staining in each group for analysis of the infarct size (left) and quantitative analysis of the infarction area/LV area and AAR/LV area ratios (right, n = 6). **(C)** Images of TUNEL (red), α-actinin (green), and DAPI (blue) staining (left) and the percentage of TUNEL-positive nuclei (right, n = 6). Scale bars = 50 μm. **(D)** qPCR analyses of Bax and Bcl2 mRNA levels in the border zone of the ischaemic heart (n = 6). The results of Bax and Bcl2 expression analysis are presented as the Bax/Bcl-2 ratio. **(E)** DHE staining of myocardial slices (left) and quantification of the ROS level (right, n = 6). Scale bar: 50 μm. **(F)** qPCR analyses of NOX4 mRNA levels in the border zone of the ischaemic heart (n = 6). **(G)** Immunoblot analysis of NRF2, Drp1 and Mfn1/2 protein levels in the border zone of the ischaemic hearts and quantification of relative protein band densities (right, n = 4). **(H)** qPCR analyses of NQO1, SOD1, Prdx1 and Gclc mRNA levels (n = 6). **(I)** Measurement of serum SOD and MDA levels by assay kits (n = 6). The data are expressed as the mean ± SEM, and n represents the number of mice in each group. (For interpretation of the references to colour in this figure legend, the reader is referred to the Web version of this article.)

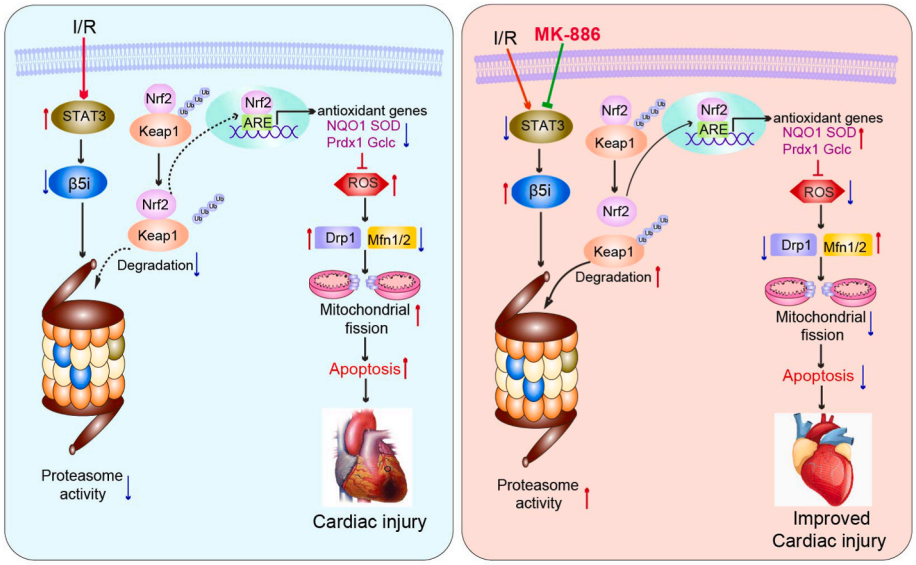

Fig. 7. A graphical abstract of the mechanism by which MK-886 meliorates cardiac I/R injury.
I/R injury activates SATA3 activity, decreasing the expression of the immunosubunit β5i and proteasome activity, which reduces the degradation of ubiquitinated keap1, leading to decreased NRF2-mediated antioxidant activity and mitochondrial fission/fusion imbalance; this contributes to cardiac apoptosis and dysfunction. In contrast, MK-886 treatment greatly reverses these effects caused by I/R insult.

inhibiting the transcription factor SATA3.

Oxidative stress is a critical factor that contributes to I/R-mediated cardiac impairment. The ROS level is dependent on a balance between the oxidant and antioxidant systems. The Keap1-NRF2-ARE axis is the most important pathway that maintains the redox balance by upregulating the expression of antioxidant enzymes (NQO1, SOD, Prdx1, and Gclc) [5,43]. Dysfunction of this axis results in excessive ROS production; this increases intracellular Ca^{2+}-dependent activation of calpain and calcineurin, which induces the dephosphorylation of Drp1, leading to increases in mitochondrial fission and ROS levels, ATP depletion and subsequent aggravation of cardiac I/R injury [44]. In addition, NRF2 is able to upregulate proteasome expression, which enhances the degradation of Drp1 [17]. Here, our data support that MK-886 treatment promotes β5i-mediated keap1 degradation and activation of NRF2, thereby ameliorating the mitochondrial fission-fusion imbalance via downregulation of Drp1 and upregulation of Mfn1/2 (Fig. 3D). This change was markedly reversed by inhibitors of the proteasome or NRF2 (Fig. 5G and 6G), suggesting that MK-886 ameliorates I/R-mediated mitochondrial dynamic imbalance though proteasome-keap1-NRF2 signalling.

Accumulating data demonstrate that keap1-NRF2 signalling exerts a protective effects in experimental models of atherosclerosis, cardiac hypertrophy, heart failure, and I/R injury [5]. Thus, modulating the activation of the Keap1-NRF2 axis is considered a therapeutic strategy for cardiac injury after I/R and myocardial infarction (MI). The E3 ligase complex (Keap1-Cul3-Rbx1) is required for the regulation of NRF2 ubiquitination and subsequent proteasomal degradation [45]. In contrast, blocking βTrCP- or Synoviolin/Hrd1-mediated ubiquitination of NRF2 attenuates its degradation [46]. In addition to NRF2 ubiquitination and degradation, an alternative mechanism regulating NRF2 protein stability has been discovered. Several ubiquitin-related enzymes, including E3 ligases (TRIM15 and TRIM25) and deubiquitinase (USP7), can regulate keap1 ubiquitin-mediated proteasomal degradation in cancer cells and cardiac tissues [20–22]. In current study, we also detected the expression levels of TRIM15, TRIM25 and USP7 in the heart at 6–72 h following I/R and found that the mRNA levels of these enzymes were not statistically different among the various time points (Fig. S3), excluding the potential involvement of these enzymes in regulating keap1 stability in the heart after I/R. Moreover, phosphorylation of p62 (also known as SQSTM1) increases its binding to Keap1 and promotes the recruitment of LC3 and autophagy induction, leading to degradation of Keap1 and activation of NRF2 signalling in the ischaemic heart [47]. In addition to endogenous factors that regulate activation of Keap1-NRF2 signalling, numerous small molecules, including natural products, have been identified as NRF2 activators. These compounds are able to limit Keap1-mediated NRF2 ubiquitination and degradation by the proteasome, which enhances NRF2-dependent upregulation of its downstream genes [4,6,43]. Previous studies have revealed that MK-866 regulates several diseases through anti-inflammatory and antioxidant activity [31–35]. Here, we provide a new mechanism by which MK-886 exerts antioxidant effects by increasing β5i-keap1-NRF2 signalling, leading to the amelioration of I/R-induced mitochondrial fission–fusion imbalance and heart dysfunction (Figs. 3–4). Conversely, blocking β5i or NRF2 abolished MK-886-mediated cardioprotection following I/R injury (Figs. 5–6). Together, our data for the first time identified that MK-886 is a new inducer of NRF2-dependent signalling that exerts its effects by enhancing β5i-mediated degradation of keap1 in the heart following I/R injury. In addition, previous data indicate that the immunoproteasome subunit β5i also targets other signalling mediators, such as IKBα–NF–kB, SOCS3, and ATG5, in several cardiac diseases. However, whether MK-886 influences the levels of these substrates in the heart after I/R needs to be tested in future studies.

5. Conclusion

Here, we have revealed a new role for MK-886 as an inducer of the immunosubunit β5i, which exerts a cardioprotective effect following I/R injury by directly targeting keap1 degradation and activating NRF2-dependent antioxidant activity *in vivo*. Our findings are of potential clinical interest, suggesting that MK-886 may be an effective agent for the prevention of I/R-mediated cardiac damage. Additional experiments are needed to identify the precise mechanism by which MK-886 enhances β2i and β5i expression in the heart, to verify the effect of MK-886 in other I/R animals, and to affirm whether MK-886 could be a new candidate for the intervention of ischemic diseases in clinical settings.

Author's contributions

KNS, PBL and HXS performed the experiments. KNS and JG performed data analysis and manuscript editing. HHL contributed to the study design, manuscript writing and editing. All authors approved the final manuscript.

Funding

This work was supported by grants from the National Natural Science

Foundation of China (No. 82030009).

Availability of data and materials

All data generated or analysed during this study are included in this published article.

Declaration of competing interest

The authors have declared that they have no conflicts of interest.

Data availability

Data will be made available on request.

Acknowledgements

None.

Appendix A. Supplementary data

Supplementary data to this article can be found online at https://doi.org/10.1016/j.redox.2023.102706.

Abbreviations

I/R	ischaemia/reperfusion
ALOX5	arachidonate 5-lipoxygenase
IL-1β	interleukin-1β
IL-6	interleukin-6
TNF-α	tumour necrosis factor alpha
ATP	adenosine triphosphate
MDA	malondialdehyde
SOD	superoxide dismutase
STAT3	signal transducer and activator of transcription 3
Keap1	Kelch-like ECH-associated protein 1
NRF2	nuclear factor erythroid 2-related factor 2
ARE	antioxidant response element
NQO1	NADPH:quinone oxidoreductase 1
GPX	glutathione peroxidase
Gclc	glutamate-cysteine ligase
Prdx1	peroxiredoxin 1
Drp1	dynamin-related protein 1
Mfn1/2	mitofusin 1/2

References

[1] M. Zhou, Y. Yu, X. Luo, J. Wang, X. Lan, P. Liu, Y. Feng, W. Jian, Myocardial ischemia-reperfusion injury: therapeutics from a mitochondria-centric perspective, Cardiology 146 (6) (2021) 781–792.
[2] S. Liu, J. Pi, Q. Zhang, Signal amplification in the KEAP1-NRF2-ARE antioxidant response pathway, Redox Biol. 54 (2213–2317) (2022), 102389 (Electronic)).
[3] A. Raghunath, K. Sundarraj, R. Nagarajan, F. Arfuso, J. Bian, A.P. Kumar, G. Sethi, E. Perumal, Antioxidant response elements: discovery, classes, regulation and potential applications, Redox Biol. 17 (2213–2317) (2018) 297–314 (Electronic)).
[4] Q.M. Chen, A.J. Maltagliati, Nrf2 at the heart of oxidative stress and cardiac protection, Physiol. Genom. 50 (2) (2018) 77–97.
[5] A. Mata, S. Cadenas, The antioxidant transcription factor Nrf2 in cardiac ischemia-reperfusion injury, Int. J. Mol. Sci. 22 (21) (2021).
[6] H.X. Li, T.H. Wang, L.X. Wu, F.S. Xue, G.H. Zhang, T. Yan, Role of Keap1-Nrf2/ARE signal transduction pathway in protection of dexmedetomidine preconditioning against myocardial ischemia/reperfusion injury, Biosci. Rep. 42 (9) (2022).
[7] Q.Y. Sun, H.H. Zhou, X.Y. Mao, Emerging roles of 5-lipoxygenase phosphorylation in inflammation and cell death, Oxid. Med. Cell. Longev. 2019 (2019), 2749173 (1942-0994 (Electronic)).
[8] D. Poeckel, C.D. Funk, The 5-lipoxygenase/leukotriene pathway in preclinical models of cardiovascular disease, Cardiovasc. Res. 86 (2) (2010) 243–253.
[9] A. Adamek, S. Jung, C. Dienesch, M. Laser, G. Ertl, J. Bauersachs, S. Frantz, Role of 5-lipoxygenase in myocardial ischemia-reperfusion injury in mice, Eur. J. Pharmacol. 571 (1) (2007) 51–54.
[10] Y.L. Zhang, P.B. Li, X. Han, B. Zhang, H.H. Li, Blockage of fibronectin 1 ameliorates myocardial ischemia/reperfusion injury in association with activation of AMP-LKB1-AMPK signaling pathway, Oxid. Med. Cell. Longev. 2022 (2022), 6196173 (1942-0994 (Electronic)).
[11] E. Gao, Y.H. Lei, X. Shang, Z.M. Huang, L. Zuo, M. Boucher, Q. Fan, J.K. Chuprun, X.L. Ma, W.J. Koch, A novel and efficient model of coronary artery ligation and myocardial infarction in the mouse, Circ. Res. 107 (12) (2010) 1445–1453.
[12] L. Kong, C. Xu, N. Sun, F. Liang, M. Wei, X. Su, [Melatonin alleviates myocardial ischemia-reperfusion injury in mice by inhibiting inflammatory response via activating Nrf2 signaling], Nan Fang Yi Ke Da Xue Xue Bao 41 (8) (2021) 1165–1170.
[13] P. Xian, Y. Hei, R. Wang, T. Wang, J. Yang, J. Li, Z. Di, Z. Liu, A. Baskys, W. Liu, S. Wu, Q. Long, Mesenchymal stem cell-derived exosomes as a nanotherapeutic agent for amelioration of inflammation-induced astrocyte alterations in mice, Theranostics 9 (20) (2019) 5956–5975.
[14] L.L. Xu, H.X. Su, P.B. Li, H.H. Li, Ursolic acid ameliorates myocardial ischaemia/reperfusion injury by improving mitochondrial function via immunoproteasome-pp2a-AMPK signalling, Nutrients 15 (4) (2023).
[15] K. Kondo, K. Umemura, T. Ohmura, H. Hashimoto, M. Nakashima, Suppression of intimal hyperplasia by a 5-lipoxygenase inhibitor, MK-886: studies with a photochemical model of endothelial injury, Thromb. Haemostasis 79 (3) (1998) 635–639.
[16] M.A. Trevethick, N.M. Clayton, A.K. Bahl, P. Strong, I.W. Harman, Leukotrienes do not contribute to the pathogenesis of indomethacin-induced ulceration of the gastric antrum in the re-fed rat, Agents Actions 41 (3–4) (1994) 179–183.
[17] R. Sabouny, E. Fraunberger, M. Geoffrion, A.C. Ng, S.D. Baird, R.A. Screaton, R. Milne, H.M. McBride, T.E. Shutt, The keap1-nrf2 stress response pathway promotes mitochondrial hyperfusion through degradation of the mitochondrial fission protein Drp1, Antioxidants Redox Signal. 27 (18) (2017) 1447–1459.
[18] Z. Zhu, W. Liang, Z. Chen, J. Hu, J. Feng, Y. Cao, Y. Ma, G. Ding, Mitoquinone protects podocytes from angiotensin II-induced mitochondrial dysfunction and injury via the keap1-nrf2 signaling pathway, Oxid. Med. Cell. Longev. 2021 (2021), 1394486 (1942-0994 (Electronic)).
[19] M. Liu, C. Zhang, X. Xu, X. Zhao, Z. Han, D. Liu, R. Bo, J. Li, Z. Liu, Ferulic acid inhibits LPS-induced apoptosis in bovine mammary epithelial cells by regulating the NF-kappaB and Nrf2 signalling pathways to restore mitochondrial dynamics and ROS generation, Vet. Res. 52 (1) (2021) 104.
[20] M. Liang, L. Wang, Z. Sun, X. Chen, H. Wang, L. Qin, W. Zhao, B. Geng, E3 ligase TRIM15 facilitates non-small cell lung cancer progression through mediating Keap1-Nrf2 signaling pathway, Cell Commun. Signal. 20 (1) (2022) 62.
[21] Y. Liu, S. Tao, L. Liao, Y. Li, H. Li, Z. Li, L. Lin, X. Wan, X. Yang, L. Chen, TRIM25 promotes the cell survival and growth of hepatocellular carcinoma through targeting Keap1-Nrf2 pathway, Nat. Commun. 11 (1) (2020) 348.
[22] Q. Xu, M. Liu, J. Gu, S. Ling, X. Liu, Z. Luo, Y. Jin, R. Chai, W. Ou, S. Liu, N. Liu, Ubiquitin-specific protease 7 regulates myocardial ischemia/reperfusion injury by stabilizing Keap1, Cell Death Dis. 8 (1) (2022) 291.
[23] S. Schlossarek, S.R. Singh, B. Geertz, H. Schulz, S. Reischmann, N. Hubner, L. Carrier, Proteasome inhibition slightly improves cardiac function in mice with hypertrophic cardiomyopathy, Front. Physiol. 5 (2014) (1664-042X (Print)):484.
[24] X. Han, Y.L. Zhang, Q.Y. Lin, H.H. Li, S.B. Guo, ATGL deficiency aggravates pressure overload-triggered myocardial hypertrophic remodeling associated with the proteasome-PTEN-mTOR-autophagy pathway, Cell Biol. Toxicol. (2022) (1573-6822 (Electronic)).
[25] H. Yao, Q. Xie, Q. He, L. Zeng, J. Long, Y. Gong, X. Li, X. Li, W. Liu, Z. Xu, H. Wu, C. Zheng, Y. Gao, Pretreatment with panaxatriol saponin attenuates mitochondrial apoptosis and oxidative stress to facilitate treatment of myocardial ischemia-reperfusion injury via the regulation of keap1/nrf2 activity, Oxid. Med. Cell. Longev. 2022 (2022), 9626703 (1942-0994 (Electronic)).
[26] K. Kitagawa, M. Matsumoto, M. Hori, Cerebral ischemia in 5-lipoxygenase knockout mice, Brain Res. 1004 (1–2) (2004) 198–202.
[27] N.S. Patel, S. Cuzzocrea, P.K. Chatterjee, R. Di Paola, L. Sautebin, D. Britti, C. Thiemermann, Reduction of renal ischemia-reperfusion injury in 5-lipoxygenase knockout mice and by the 5-lipoxygenase inhibitor zileuton, Mol. Pharmacol. 66 (2) (2004) 220–227.
[28] O.O. Lisovyy, V.E. Dosenko, V.S. Nagibin, L.V. Tumanovska, M.O. Korol, O. V. Surova, O.O. Moibenko, Cardioprotective effect of 5-lipoxygenase gene (ALOX5) silencing in ischemia-reperfusion, Acta Biochim. Pol. 56 (4) (2009) 687–694.
[29] S. Gautam, S. Roy, M.N. Ansari, A.S. Saeedan, S.A. Saraf, G. Kaithwas, DuCLOX-2/5 inhibition: a promising target for cancer chemoprevention, Breast Cancer 24 (2) (2017) 180–190.
[30] C.A. Rouzer, A.W. Ford-Hutchinson, H.E. Morton, J.W. Gillard, MK886, a potent and specific leukotriene biosynthesis inhibitor blocks and reverses the membrane association of 5-lipoxygenase in ionophore-challenged leukocytes, J. Biol. Chem. 265 (3) (1990) 1436–1442.
[31] P. Provost, P. Borgeat, Y. Merhi, Platelets, neutrophils, and vasoconstriction after arterial injury by angioplasty in pigs: effects of MK-886, a leukotriene biosynthesis inhibitor, Br. J. Pharmacol. 123 (2) (1998) 251–258.
[32] F.G. Al-Amran, N.R. Hadi, H.S. Al-Qassam, Effects of thyroid hormone analogue and a leukotrienes pathway-blocker on reperfusion injury attenuation after heart transplantation, ISRN Pharmacol 2013 (2013), 303717 (2090-5165 (Print)).
[33] N.F. Voelkel, R.M. Tuder, K. Wade, M. Hoper, R.A. Lepley, J.L. Goulet, B.H. Koller, F. Fitzpatrick, Inhibition of 5-lipoxygenase-activating protein (FLAP) reduces pulmonary vascular reactivity and pulmonary hypertension in hypoxic rats, J. Clin. Invest. 97 (11) (1996) 2491–2498.
[34] N.R. Hadi, F.G. Al-amran, A.A. Hussein, Effects of thyroid hormone analogue and a leukotrienes pathway-blocker on renal ischemia/reperfusion injury in mice, BMC Nephrol. 12 (1471–2369) (2011) 70 (Electronic)).

[35] G. Daglar, T. Karaca, Y.N. Yuksek, U. Gozalan, F. Akbiyik, C. Sokmensuer, B. Gurel, N.A. Kama, Effect of montelukast and MK-886 on hepatic ischemia-reperfusion injury in rats, J. Surg. Res. 153 (1) (2009) 31–38.
[36] M. Basler, M. Groettrup, On the role of the immunoproteasome in protein homeostasis, Cells 10 (11) (2021).
[37] X. Xie, H.L. Bi, S. Lai, Y.L. Zhang, N. Li, H.J. Cao, L. Han, H.X. Wang, H.H. Li, The immunoproteasome catalytic beta5i subunit regulates cardiac hypertrophy by targeting the autophagy protein ATG5 for degradation, Sci. Adv. 5 (5) (2019), eaau0495.
[38] W. Yan, H.L. Bi, L.X. Liu, N.N. Li, Y. Liu, J. Du, H.X. Wang, H.H. Li, Knockout of immunoproteasome subunit beta2i ameliorates cardiac fibrosis and inflammation in DOCA/Salt hypertensive mice, Biochem. Biophys. Res. Commun. 490 (2) (2017) 84–90.
[39] J. Li, S. Wang, J. Bai, X.L. Yang, Y.L. Zhang, Y.L. Che, H.H. Li, Y.Z. Yang, Novel role for the immunoproteasome subunit PSMB10 in angiotensin II-induced atrial fibrillation in mice, Hypertension 71 (5) (2018) 866–876.
[40] J. Li, S. Wang, Y.L. Zhang, J. Bai, Q.Y. Lin, R.S. Liu, X.H. Yu, H.H. Li, Immunoproteasome subunit beta5i promotes ang II (angiotensin II)-Induced atrial fibrillation by targeting ATRAP (ang II type I receptor-associated protein) degradation in mice, Hypertension 73 (1) (2019) 92–101.
[41] F.D. Li, H. Nie, C. Tian, H.X. Wang, B.H. Sun, H.L. Ren, X. Zhang, P.Z. Liao, D. Liu, H.H. Li, Y.H. Zheng, Ablation and inhibition of the immunoproteasome catalytic subunit LMP7 attenuate experimental abdominal aortic aneurysm formation in mice, J. Immunol. 202 (4) (2019) 1176–1185.
[42] A. Angeles, G. Fung, H. Luo, Immune and non-immune functions of the immunoproteasome, Front. Biosci. 17 (5) (2012) 1904–1916.
[43] W.D. Hedrich, H. Wang, Friend or foe: xenobiotic activation of Nrf2 in disease control and cardioprotection, Pharm. Res. (N. Y.) 38 (2) (2021) 213–241.
[44] M.S. Shah, M. Brownlee, Molecular and cellular mechanisms of cardiovascular disorders in diabetes, Circ. Res. 118 (11) (2016) 1808–1829.
[45] J. Vriend, R.J. Reiter, The Keap1-Nrf2-antioxidant response element pathway: a review of its regulation by melatonin and the proteasome, Mol. Cell. Endocrinol. 401 (1872–8057) (2015) 213–220 (Electronic)).
[46] B. Harder, T. Jiang, T. Wu, S. Tao, M. Rojo de la Vega, W. Tian, E. Chapman, D. D. Zhang, Molecular mechanisms of Nrf2 regulation and how these influence chemical modulation for disease intervention, Biochem. Soc. Trans. 43 (4) (2015) 680–686.
[47] W. Zhang, C. Feng, H. Jiang, Novel target for treating Alzheimer's Diseases: crosstalk between the Nrf2 pathway and autophagy, Ageing Res. Rev. 65 (1872–9649) (2021), 101207 (Electronic)).